Green-state micromilling of AISI316L feedstock

WCMNM
2017
No.

Parenti Paolo[1], Kuriakose Sandeep[1], Mussi Valerio[2], Strano Matteo[1], Annoni Massimiliano[1]

[1]*Politecnico di Milano, Department of Mechanical Engineering, 20156, Milan, Italy*
[2]*Laboratorio MUSP, 29122, Piacenza, Italy*

Abstract

Powder metallurgy offers products characterized by unique properties and minimum material waste. However, the deformation in debinding and sintering phases and the limited attainable surface finish, may requires additional manufacturing steps for enabling high-quality components production. Recent developments in micro components fabrication by extrusion and in extrusion-based additive manufacturing, have been trying to adopt metal polymeric feedstock for producing high-end components for biomedical and other relevant industrial fields. At the same time, to enhance product quality these manufacturing process chains requires the integration at different phases of machining operations. This paper studies the micromachinability of AISI316L feedstock at green-state, aiming on geometrical features obtained on hot-pressed discs, by using a 0.5 mm diameter end-mill. The work analyzes the effect of pressing parameters combined with machining parameters on surface roughness and integrity of machined slots. 3D microscopy and cutting force acquisition were adopted. Quality of sintered components were also analyzed. Machinability of green parts resulted limited, especially considering the achievable roughness and the damages occurred at slot edges. However, proper combination of cutting parameters led to better results indicating that potential benefits can be achieved. On the other side, debinding and sintering phases confirmed as critical phases that can potentially invalidate the production of good components but their performance seemed not compromised by previous micromilling operations.

Keywords: micromilling, process chain, powder metallurgy, surface quality, AISI 316L feedstock.

1. Introduction

Powder metallurgical products are widely growing in numbers and applications because of the cost savings of powder metallurgical processes compared with alternative processes and matchless properties achievable only by them. A generic process chain consists in: 1) mixing of metal powders with polymeric binder to form a homogeneous feedstock, 2) generation of desired components geometry at green-state using different manufacturing techniques, 3) debinding and drying using water, solvent and/or thermal treatments, 4) sintering to reach the required final properties [1-2]. In addition to hard materials like ceramic and tungsten carbide, nowadays powder metallurgy is used for fabrication of standard metallic component using metal injection moulding and hot pressing [2]. Most recently, extrusion also evolved as a promising methodology for the development of innovative additive manufacturing (AM) process chain, exploiting powder metallurgical principle [3]. The main problems faced in fabrication and microfabrication of powder metallurgical products are the geometry variation due to the shrinkage and defects caused by debinding and sintering [4]. In the AM scenario, micro machining can be very effective to compensate geometrical inaccuracy and to increase surface finish of the deposited part, especially to surfaces that will not be accessible at the end of the deposition process [3, 5]. Feedstock machining at green-state, i.e. before debinding and sintering can be adopted for cost-saving, thanks to a better machinability because of low mechanical material strength [6] or because it allows to compensate the subsequent predictable part distortion [7]. This research work investigates the possibility of integrating micromilling in a potential AISI316L powder metallurgical process chain. Rather than going directly for the AM chain, in this study, hot pressed discs are micromachined to provide general machinability indications of green-state AISI316L feedstock.

2. Method

Hot pressing was adopted in this study to obtain the green-state specimens. Pressing was chosen since it gives the most homogeneous material structures, especially comparing to the other mentioned extrusion based methods.

Feedstock material was produced in-house starting from commercially available gas atomized sperical powder of AISI316L with nominal median particle size = 50 µm. A 25%vol polymeric binder SILIPLAST HE was adopted at mixing temperature of 140 °C for 5 min. Feedstock material was hot pressed at constant temperature of 130°C into circular discs with an approximate diameter of 30 mm and thickness 3.95 mm, by means of Imptech M 10 mounting press. Experiments were conducted at two pressure levels 20 MPa and 40 MPa by keeping holding and cooling time to 10 min and 7.5 min, respectively [8].

Four Specimens, named “Sample A” and “Sample C” (Pressure 20 MPa) and “Sample B” and “Sample D” (Pressure 40 MPa) were prepared for the two pressure levels and milling experiments were conducted with two repetitions.

Micro slots were obtained on the green samples by using Kern EVO 5-axis CNC machining centre (Fig. 1). Samples were fixed on a work base, attached to a

triaxial dynamometer Kistler 9317 working at @ 51,2 KHz, by using hot glue to limit part damage (Fig. 1). Cutting Forces were first compensated to filter out the pure dynamic behaviour of the sensor and the electrical-thermal derive, and were post-processed to produce the resultant force computation in the X-Y-Z plane, i.e. *Fr*, whose RMS value was computed using Matlab® and plotted using Minitab®.

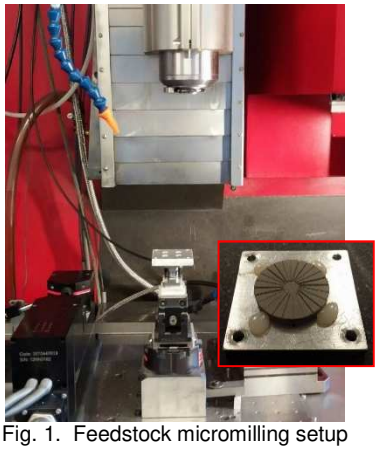

Fig. 1. Feedstock micromilling setup

A radial slot pattern was adopted on the specimens, with 24 multiple slots on each sample (15° degree of angular shift). A central circular pocket with a diameter of 6 mm and 0,3 mm depth was firstly milled to simplify micro mills entrance on the slots.

Micro flat end mills (Sandvik R216.32-00530-AE05G1620) with 0,5 mm and 2 teeth were adopted in full slot cutting (radial depth of cut equal to mill diameter i.e. 0,5 mm). The other parameters and levels were selected based on preliminary tests and experience and on previous literature works [7,9]. They were cutting speed (vc), feed per tooth (fz) and axial depth of cut (ap), Table. 1. Therefore, 24 experiments were conducted on each specimen for a total of 96 cuts/slots. No assisting air was used during cutting but it was adopted for cleaning the samples after cutting (low air pressure was adopted to preserve the surface integrity).

Table 1
Selected Micromilling parameters

Parameter	Low	High
Cutting speed (vc [m/min])	26	78
Feed per tooth (fz [mm/tooth])	0,016	0,048
Depth of cut (ap [mm])	0,1	0,3

The machined micro slots were analysed using optical profilometer (Mitutoyo quick vision pro) and a 3D interferometer/confocal microscope (Mahr Surf CWM 100). The latter produces accurate parts measurement including the areal surface roughness measurements on the machined slots, that adopted the arithmetic mean height, i.e. *Sa,* as synthetic indicator for quantitative roughness analysis. Computation of *Sa* was conducted by averaging three areas along the slot length (each having a size of 350 µm x 350 µm). Only form removal fitting was applied prior to *Sa* computation.

3. Results and Discussion

3.1 Samples preparation

Visual samples inspection after pressing showed good homogeneity of all the specimens that were apparently well compacted. Small surface integrity defects and augmented porosity affected some little areas on the upper disc surfaces (all the four discs), most likely due to binder adhesion on the pressing punch. In addition, few integrity defects evenly distributed on the disc perimeter affected upper disc external edge of samples B and D. Apart from that, the obtained samples were suitable for conducting machining experiments.

3.2 Machining operations

Overall samples integrity was preserved during cutting and all the slots were created according to the programmed toolpath. Fig. 2 shows two of the four produced samples. After chip formation, the removed material showed a tendency to form relatively big agglomerates around the cutting area, posing the need to evacuate them properly. Nevertheless, tool tip geometry appeared clean at the end of all the cutting passes. This apparently confirmed a low adhesion tendency of the chip on the tool faces (i.e. no built-up-edge, or similar phenomena). As expected from the very limited contact time (around 10 s for each sample) and the low hardness of the samples material, no noticeable tool wear was observed at the end of the cutting.

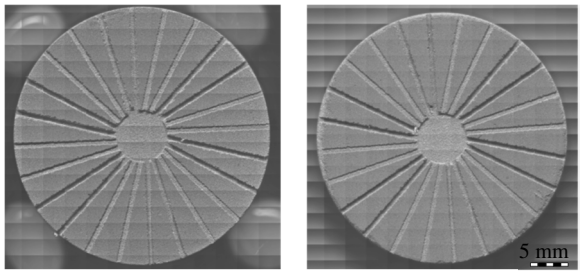

Fig. 2. Sample A and Sample B after machining

3.2.1 Force Analysis

Resultant Cutting forces maintained at low levels, lower than 1,5 N of RMS value, confirming the high machinability of green feedstock (Fig.3). Cutting parameters played a role, partly covered by the high variability of *Fr* among the replicates, showing an atypical behavior in comparison to bulk AISI316L metal machining. Axial depth of cut, for instance, did to not play a proportional role on the force, as instead is typical in bulk metals, due to the specific removal mechanism occurring during feedstock micromachining. Feed per tooth and cutting speed played a minor and opposite role, with this latter leading to a decrease of *Fr* RMS values, most likely due to the cutting temperature effect on the material characteristics (thermal softening acting on the binder). On the other side, pressure used to obtain the samples seemed to not make any statistical difference on *Fr*.

3.2.2 Part Accuracy and Surface Quality

Eye samples inspection showed an overall

homogeneity of the machined slots, but microscope analysis put in evidence relevant variations and different integrity defects affecting samples surfaces.

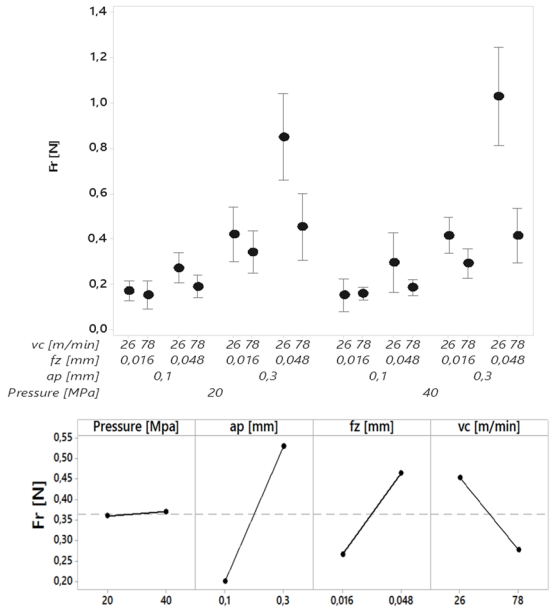

Fig. 3. Resultant cutting Force *Fr* analysis

First, deviations in the actual depth of the slots were noticed for all the samples with overall overcutting errors up to 23% among the slots (i.e. a slot with ap=300 µm had an actual machined depth of 360 µm) as depicted in Fig. 4.

About the achieved roughness, micromilling reduced the surface quality in respect to the originally pressed surfaces (characterized by a *Sa* in the order of 5 µm). The average slot roughness assumed values around 11 µm and no relevant variations were observed along the slots length.

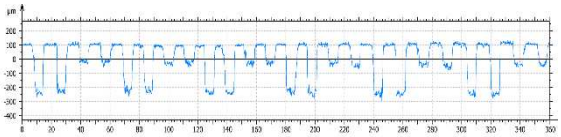

Fig 4. Slots profile on Sample A at a diameter = 10 mm

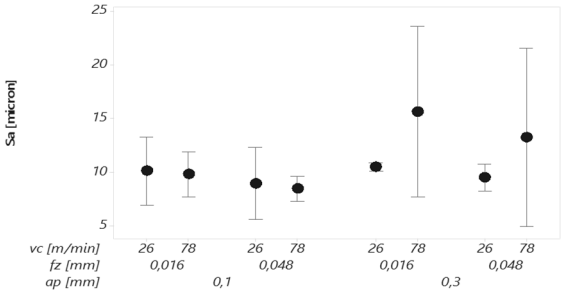

Fig. 5. Roughness values of Sample A

On the other side, big variability was shown among the replicates, especially when higher ap and vc were adopted on the samples (Fig.5). Eventually in some cases, the slots were affected by big irregularities caused by teared material and fragments not perfectly removed by the cutting action, which generated abnormally high values of *Sa* (bigger than 20 µm).

From the surface and geometrical integrity point of view, three main defects were classified: 1) those affecting the upper slot edges (quantified as the difference between W_{nom} and W_{act}, see Fig. 6), 2) those at the slot entrance where thin walls were generated by the toolpath (quantified as Δb, see Fig. 6) and 3) those at the slot exit. All these defects resulted governed by cutting parameters in a similar way among the cutting replicas.

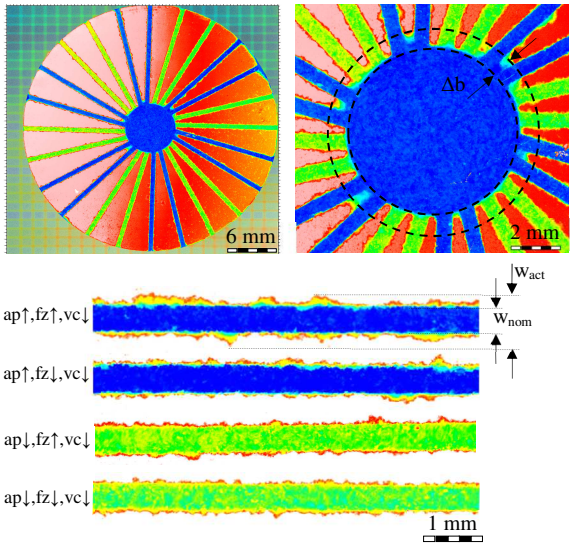

Fig 6. Integrity defects of sample A

Adopting lower vc and ap, showed on all the samples better slot edge integrity than higher vc and ap values. Increasing the feed per tooth value also affected the edge quality by worsening the localized defects. This trend was same in both specimen A hot pressed for 20 MPa and B for 40 MPa.

Similar results were showed by the defects at the slot exit zone, characterized by an almost symmetric wedge-shaped overcut. The amplitude of this defect followed the same trend as the upper edge integrity defects and in few cases led to a partial collapse of the sample border (W_{act} up to 2,8 mm, Fig. 6).

Conversely, the integrity of the entrance slots zone was evaluated at the end of the machining operation and therefore the showed results were coupled for two adjacent slots. Mostly all the thin walls, formed at the slot entry with nominal width of 0,285 mm), resulted broken between two slots machined with the harshest depth conditions (i.e. ap=0,3). The collapse of the material gave geometrical errors i.e. Δb_{max}=1,08 mm. Oppositely, mostly all the slots machined with lower ap and fz were almost intact (Δb_{max}<0,3 mm). Effect of sample pressure on Δb was not statistical significant.

3.3. Debinding / Sintering

Two green feedstock specimens (sample C and D) were debinded and sintered to study the effect on the micro milled slots characteristics and the actual integrability of micromilling into the process chain. Samples were firstly dipped in solvent and demineralized agitated water with 2%vol of Inhibitor 4000 at 70°C for 24 hours. In this phase expulsion of air entrapped in the samples was showed, especially for sample C. Air entrapment porosity, did not form close to machined slots and caused minor damages

on the upper sample surfaces, reflecting on final samples quality after sintering.

Specimens were directly dried for two hours at 100°C in air convection furnace by avoiding furnace debinding (because of the nature of polymeric debinder). Sintering was carried out in tubular furnace in argon flux (150 l/h) by using the temperature law shown in Table 2.

Table 2
Debinding and sintering temperature profile for feedstock AISI316L with 25% SILIHE binder

Start (°C)	End (°C)	Time (hh:mm)	Ramp (°C/h)
20	400	7:30 + 1:00 (hold)	50
400	450	1:00 + 1:00 (hold)	50
450	1360	5:00 + 1:00 (hold)	180
1360	1000	2:00	-180
1000	20	Natural cooling	

After sintering the specimens presented different surface morphology, Fig. 7. In this study, the shrinkage and overall geometrical sample deformations were not investigated since there were not the research focus. On one side sample C, pressed at 20 MPa, developed a wide peel off integrity defect, close to the specimen center, easiliy visible in the picture, Fig. 7. The morphology of this defects tell that it was probably originated by subsurface damages or cracks already generated at the pressing stage and not during micromilling operations. On the opposite, Sample D, pressed at 40 MPa showed good homogeneity wothout any additional defects associable with the green-state slot micromilling.

Fig. 7 Sample C and Sample D after sintering

5. Conclusions

This research studied the machinability of green-state AISI316L feedstock in order to evaluate the actual potential of integrating micromilling into the process chain for fabrication of metallic parts from metal polymer feedstock. The analysis conducted on the AISI316L feedstock (in-house produced with a specific recipe) proved that micromilling can be used to produce on this material only rough features. The very low developed cutting forces showed sensitivity with respect to cutting parameters, in a dissimilar way comparing to bulk metal machining. This puts in evidence the different cutting mechanism involved when micromilling this material.

Integrity of the slot upper borders were strongly affected by cutting conditions meaning that parameter selection play an important role for the success of micromilling integration into the process chain. In particular, lower depth of cut with high cutting speed and low feed per tooth led to better slot integrity.

Achievable surface finish and roughness of green-state feedstock resulted limited but increased during sinterization process.

In this preliminary study, pressing did not affected the green machinability in a relevant way even if some small effects were observed on sample integrity. However, pressure played a big role on the samples sinterizability confirming that all the steps of the process chain are interconnected and should be properly governed to produce good components.

Acknowledgements

This research work was undertaken in the context of MICROMAN project (“Process Fingerprint for Zero-defect Net-shape MICROMANufacturing”, http://www.microman.mek.dtu.dk/). MICROMAN is a European Training Network supported by Horizon 2020, the EU Framework Programme for Research and Innovation (Project ID: 674801). Thanks go also to Mr. Covelli and Mr. Atta for their support with experimental setup and experiments.

References

[1] J. Li et al., “Micro machining of pre-sintered ceramic green body,” J Mater Process Tech 2012; 212:571–579. doi:10.1016/j.jmatprotec.2011.10.030.

[2] K.H. Kate et al., “Simulations and injection molding experiments for aluminum nitride feedstock,” Ceram Int 2016; 42:194–203. doi:10.1016/j.ceramint.2015. 08.079.

[3] M. Annoni et al., “Feasibility study of an extrusion - based direct metal additive manufacturing technique”. Procedia Manuf 2016; 5: 916–927. doi:10. 1016/j.promfg.2016. 08.079.

[4] S. Dhara et al., “Green machining to net shape alumina ceramics prepared using different processing routes,” Int. J. Appl. Ceram. Technol., 2 2005; 3: 262–270.

[5] W. Du et al., “A novel method for additive / subtractive hybrid manufacturing of metallic parts,” Procedia Manuf 2016; 5:1018–1030. doi:10. 1016/j. promfg.2016.08.067.

[6] E. Robert-perron et al., “Machinability of green powder metallurgy components: part I. characterization of the influence of tool wear,” Metallurgical and materials transactions A 2007; 38A: 1330-1336.

[7] G. Bukvic et al., “Green machining oriented to diminish density gradient for minimization of distortion in advanced ceramics”. Machining Science and Technology 2012; 16:2, 228-246. doi:10.1080/10910344. 2012.673968.

[8] A. Celik. et al., “Effect of heat treatment on green machinability of SiAlON compacts,” J Mater Process Tech 2014; 214: 767–774. doi:10.1016/j.jmatprotec.2013.11.019.

[9] S.H. Ng et al., “Machining of novel alumina / cyanoacrylate green ceramic compacts,” J Mater Process Tech 2006; 175: 299–305.